

Nonmonotonic swelling and compression dynamics of hydrogels in polymer solutionsFrank J. Aangenendt,^{1,2,3,*} Melle T. J. J. M. Punter^{4,*} Bela M. Mulder,⁴ Paul van der Schoot,^{5,6} and Hans M. Wyss^{1,2,3,†}¹*Department of Mechanical Engineering, Materials Technology, Eindhoven University of Technology, 5600MB Eindhoven, Netherlands*²*Institute for Complex Molecular Systems, Eindhoven University of Technology, 5600MB Eindhoven, Netherlands*³*Dutch Polymer Institute (DPI), P.O. Box 902, 5600AX Eindhoven, Netherlands*⁴*AMOLF, Theory of Biomolecular Matter, Science Park 104, 1098XG Amsterdam, Netherlands*⁵*Department of Applied Physics, Eindhoven University of Technology, 5600MB Eindhoven, Netherlands*⁶*Department of Physics, Utrecht University, 3584CC Utrecht, Netherlands*

(Received 22 July 2020; accepted 23 September 2020; published 9 December 2020)

Hydrogels are sponge-like materials that can absorb or expel significant amounts of water. Swelling up from a dried state, they can swell up more than a hundredfold in volume, with the kinetics and the degree of swelling depending sensitively on the physicochemical properties of both the polymer network and the aqueous solvent. In particular, the presence of dissolved macromolecules in the background liquid can have a significant effect, as the macromolecules can exert an additional external osmotic pressure on the hydrogel material, thereby reducing the degree of swelling. In this paper, we have submerged dry hydrogel particles in polymer solutions containing large and small macromolecules. Interestingly, for swelling in the presence of large macromolecules we observe a concentration-dependent overshoot behavior, where the particle volume first continuously increases toward a maximum, after which it decreases again, reaching a lower, equilibrium value. In the presence of smaller macromolecules we do not observe this intriguing overshoot behavior, but instead observe a rapid growth followed by a slowed-down growth. To account for the observed overshoot behavior, we realize that the macromolecules entering the hydrogel network not only lead to a reduction of the osmotic pressure difference, but their presence within the network also affects the swelling behavior through a modification of the solvent-polymer interactions. In this physical picture of the swelling process, the net amount of volume change should thus depend on the magnitudes of both the reduction in osmotic pressure and the change in effective solvent quality associated with the macromolecules entering the pores of the hydrogel network. We develop a phenomenological model that incorporates both of these effects. Using this model we are able to account for both the swelling and compression kinetics of hydrogels within aqueous polymer solutions, as a function of the size of the dissolved macromolecules and of their effect on the effective solvent quality.

DOI: [10.1103/PhysRevE.102.062606](https://doi.org/10.1103/PhysRevE.102.062606)**I. INTRODUCTION**

Hydrogels are sponge-like materials that can absorb or expel large amounts of water. These polymer networks, which obtain the ability to absorb water from their hydrophilic functional groups and their mechanical stability from physical or chemical crosslinks, react to a wide range of stimuli and are therefore used in many academic and industrial applications. For example, hydrogel particles play an important role in medical applications where, because their mechanical properties are similar to those of biological tissue, they are used in tissue engineering [1]. Moreover, their propensity to swell or deswell under different physicochemical conditions can be exploited to control the release of drugs through the pores of the polymer network [2,3]. Hydrogels are also used in situations where an even more pronounced volume change is desirable, e.g., for water absorption and storage in personal care products or in soil improvement [4,5].

The rate at which they can change their volume depends sensitively on the typical pore size of the hydrogel

network, which affects both the permeability and the compression behavior of the gel network. A range of different theoretical treatments for describing the kinetics of these swelling/deswelling processes have been formulated, which offer slightly different definitions for the relevant material properties. Tanaka and Fillmore have formulated an equation of motion for the polymer network, where the solvent is treated as stationary [6], whereas other models, based on Biot's poroelastic consolidation theory [7], specifically take the solvent displacement into account, using coupled equations of motion for the polymer network and the solvent [8–11].

Following the viewpoint of Tanaka and Fillmore [6], a compressive modulus K for the gel network can be defined, which characterizes the elastic response to changes in the volume of the gel network. The permeability κ quantifies the ease with which a liquid can be pressed through a porous material. The product of K and κ , divided by the coefficient of friction, gives rise to the diffusion constant for the gel network, which quantifies the deformation rate of a hydrogel network in swelling and compression.

A common method for determining the compressive modulus of hydrogel particles is to perform an osmotic compression

*These authors contributed equally to this work.

†H.M.Wyss@tue.nl

measurement in which a particle is exposed to a solution of an osmolyte such as dextran [12].

This method generally relies on the assumption that the osmolytes are too large to readily enter the pores of the network, in which case a distinct osmotic pressure difference is established between the inside and the outside of the particle and, as a result, the compressive elastic modulus (i.e., the *osmotic modulus*) can be extracted directly from the equilibrium volume as a function of the applied osmotic pressure.

However, depending on the ratio between the pore size and the size of the osmolyte, the osmolyte can eventually still penetrate the hydrogel, which effectively lowers the externally applied osmotic pressure. Interestingly, such a delayed pressure reduction can lead to a complete reswelling after an initial compression, as shown in our previous experiments on microscopic polyacrylamide hydrogel particles [13]. The results of this previous study suggest that if macromolecules are able to penetrate the pores of the particle network, the compressive modulus can no longer be extracted directly from the equilibrium particle volume, without specifically taking into account the penetration of osmolyte molecules into the particle.

For the materials used in that study, however, the presence of small osmolyte macromolecules did not seem to affect the equilibrium swelling volume of the particles. Instead, upon penetration of the osmolyte into the network, the particles regained their initial volumes. This appeared to suggest that in the final equilibrium state the osmotic pressure inside and outside the particle was the same, and that the osmolyte did not significantly interact with polymer network within the particle.

However, it is known that in general, the presence of dissolved (macro)molecules in the background liquid can, in addition to osmotic pressure effects, have a significant influence on the effective solvent quality of that liquid with respect to the hydrogel network [14]. This means that the interactions between the liquid and the polymer chains in the hydrogel network can be modified by the dissolved osmolyte macromolecules, which should directly affect the network's equilibrium volume after swelling. This is somewhat analogous to the effect ions can have on polyelectrolyte gels [15–17]. Macromolecules, however, due to their larger size, diffuse significantly slower than do ions. Therefore the change in effective solvent quality associated with the macromolecules entering the gel network is expected to occur in a more delayed fashion. While such effects should clearly be considered in describing the (de)swelling kinetics of hydrogels in polymer solutions, they have often been neglected in previous studies. While the effects of solvent changes such as those induced by changes in pH, salt concentration, or by solvent exchange have been studied in detail [15,17–22], the impact of macromolecules dissolved in the background liquid on the swelling kinetics have been studied less extensively. A number of studies have considered the effects of high molecular weight macromolecules that do not enter into the hydrogel, thus leading to an additional external osmotic pressure which compresses the hydrogel network [12,18]. However, the general effects of dissolved polymers that can partly or fully penetrate a hydrogel network have not been studied as thoroughly. As a result, a full understanding of

the (de)swelling of hydrogels in polymer solutions is still lacking.

In this paper, we study experimentally and describe theoretically the swelling behavior of hydrogel particles immersed in polymer solutions. We study the kinetics of swelling, starting from a dried, compressed state, up to a fully swollen state, as a function of the concentration and molecular weight of macromolecules dissolved in the background liquid. Using macroscopic sodium polyacrylate hydrogel spheres as model hydrogel materials, we find a qualitatively new swelling behavior for swelling in the presence of macromolecules, as compared to swelling in pure solvent.

Namely, we observe an intriguing *overshoot behavior*, where after an initially rapid swelling process, the particle volume reaches a maximum at intermediate times, after which it decreases continuously to eventually reach a lower, equilibrium volume. If these hydrogel particles are swollen in solutions without added macromolecules, such an overshoot is not observed.

In addition, we also study the compression behavior of our hydrogels as they are exposed to an osmotic shock, which we induce by placing fully swollen hydrogel particles into similar polymer solutions. In agreement with our previous work [13], we find that an initial compression of the particles can be followed by a slow reswelling. In contrast to those findings, however, here we observe that, depending on the type and size of osmolyte macromolecules present in the background liquid, particles do not always fully reswell to their initial volume. Instead, they can slowly swell back to an equilibrium volume that is significantly lower than at the initial stage.

We hypothesize that both these effects, the overshoot in the swelling of the hydrogels, as well as the lack of full reswelling to the initial particle volume in a compression experiment, are due to a combination of changes in the effective solvent quality, brought about by the presence of the penetrating macromolecules within the network, and the osmotic pressure difference between the inside and the outside of the hydrogel, due to equilibrium partitioning of the osmolyte.

We describe the observed overshoot behavior during swelling, as well as the partial reswelling during compression with a simple phenomenological model that takes into account the influence of the dissolved macromolecules on both the applied osmotic pressure difference and the effective solvent quality of the background liquid and polymer inside the pores of the gel network. By incorporating these two effects, our model is able to account for both the swelling and compression kinetics of hydrogels within aqueous polymer solutions.

II. MATERIALS AND METHODS

A. Materials

We use commercially available “aquapearls” (sodium polyacrylate hydrogel particles, Deco-Boulevard, Lohmar, Germany), intended for decorative purposes, as model hydrogel particles. The material is provided as dry spheres with an average radius of $R_{\text{dry}} \approx 1.21$ mm. Submersed in water, these hydrogel particles can swell up to over 100 times their original volume.

We use polymer solutions of the following macromolecules (from small to large): dextran 70k (from *Leuconostoc* spp,

$M_w = 70$ kDa, Sigma-Aldrich, radius of gyration $R_g \approx 6$ nm [23]), polyethylene glycol 20k, (PEG 20k, $M_w = 20$ kDa, Sigma-Aldrich, $R_g \approx 7$ nm [24]), and the bigger polyethylene oxide 200k (PEO 200k, $M_w = 200$ kDa, Sigma-Aldrich, $R_g \approx 22$ nm [24]). Chemically, PEG 20k and PEO 200k are the same and only differ in molecular weight and hence chain length. For simplicity, we will refer to a “saline solution” when we use a 100 mM NaCl solution (NaCl, Sigma Aldrich, dissolved in MilliQ deionized water). We did not use any other salts or salt concentrations.

B. Methods

For both the swelling and compression experiments, sample vials containing the hydrogel particles are placed on a roller bank (Stuart Scientific SRT1, Sigma-Aldrich) to enforce a homogeneous osmolyte concentration around the particle. The kinetics of compression is in fact slightly different for the case of a particle immersed in a polymer solution without any stirring, as shown in Fig. 6 (Appendix A). In the absence of stirring, the diffusion of macromolecules outside the particle also plays an important role, while for a stirred solution it is reasonable to assume a constant concentration of osmolyte macromolecules in the surrounding solution, near the particle surface.

We measure the weight of the (de)swelling particles periodically, by removing them from the solution, and weighing them on a microbalance after carefully removing any excess surface water with tissue paper. As we know the initial mass and volume, we calculate the volume of the particle based on the measured weight, assuming that the density of water remains unchanged upon entering the hydrogel network.

Swelling is investigated by submerging a dry particle, of which we measured the initial weight and radius, in a (polymer) solution. We used a saline solution, and saline solutions to which we added 2, 4, 5, 7.5, and 10 wt % of PEO 200k, respectively. To test the influence of the smaller osmolytes we used saline solutions with 8 wt% of PEG 20k or 8 wt % dextran 70k.

Deswelling is investigated by submerging a particle that was previously swollen in a saline solution for at least a week, in a saline solution to which 4, 7.5, or 10 wt % of PEO 200k is added, respectively. We also tested saline solutions to which the smaller dextran 70k or PEG 20k has been added, both at 8 wt%.

In both swelling and deswelling experiments, each particle is immersed in a volume of background fluid that is at least a factor 50 larger than the volume of a fully swollen hydrogel particle. Moreover, the solutions were continuously stirred during the swelling and deswelling process, ensuring a homogeneous concentration of polymer chains within the background liquid. For these reasons, in our modeling we assume a constant and homogeneous osmolyte concentration in the background liquid, outside of the hydrogel particles.

III. RESULTS AND DISCUSSION

A. Swelling

As a first test of the influence of macromolecules on the swelling of hydrogels, we place a dry hydrogel particle, with

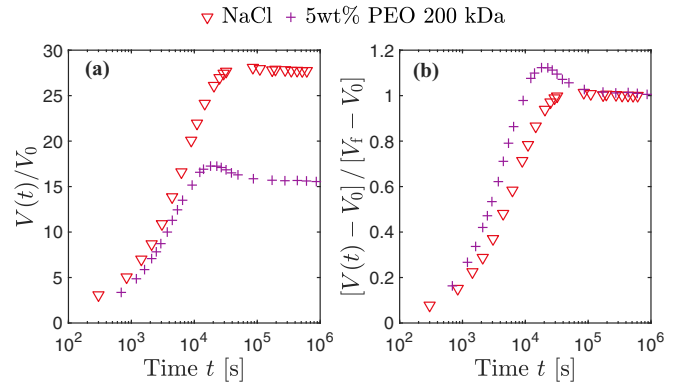


FIG. 1. Overshoot behavior: Swelling in the presence and absence of PEO 200k osmolyte. (a) Normalized hydrogel volume $V(t)/V_0$ as a function of time (see top legend). In the PEO 200k solution, a distinct overshoot in the hydrogel volume is observed, whereas in a pure NaCl solution the volume increases continuously. (b) The same data plotted in a rescaled fashion to better visualize the relative overshoot.

volume V_0 , in a saline solution and measure its increasing weight over time, which we compare to that of a particle swollen in a saline solution containing 5 wt % PEO 200k, as shown in Fig. 1(a).

Surprisingly, for the experiment in the PEO 200k solution, instead of only obtaining a reduced final volume V_f as a result of the applied osmotic pressure, we also observe a significant overshoot in the volume. To better visualize this overshoot we also plot the same data in a rescaled fashion in Fig. 1(b), as $\frac{V(t) - V_0}{V_f - V_0}$.

Interestingly, similar overshoot behavior has previously been reported [25,26] for cases where hydrogels were swollen in solutions of different pH or different ion content, monovalent versus multivalent ions for example. While some authors have attributed such overshoot behavior to dynamic conformational changes of the polymer chains within the network, the behavior is still not fully understood. However, we believe that this type of overshoot behavior is quite different from the case studied here, where no ionic or pH gradients are involved.

A possible explanation for the overshoot behavior observed here is that the PEO 200k used exhibits a significant polydispersity, implying that a fraction of the polymer could still be small enough to penetrate the hydrogel network and thereby change the effective solvent quality.

Indeed, the PEO 200k polymer used here is synthesized by suspension polymerization, which generally yields a broad molecular weight distribution. For the high molecular weight polymer considered here, this would imply a degree of polymerization close to unity and a polydispersity index $PDI = M_w/M_n \approx 2$. The distribution is expected to follow a Flory-Schulz distribution of molecular weights, which in our case would imply for instance that approximately 9 wt % (or 39% of the number of chains) of the total polymer would be chains with a molecular weight below 50 kDa, small enough to penetrate the gel network relatively swiftly.

In experiments where we only use the smaller PEG 20k, we do not observe any overshoot, and also for dextran 70k, this overshoot is not observed, as depicted in Fig. 2. However, we

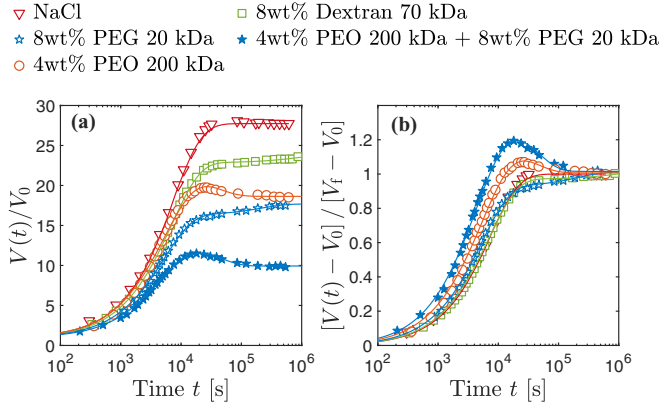


FIG. 2. Swelling in osmolyte solutions of different molecular weight. (a) Normalized hydrogel volume $V(t)/V_0$ as a function of time in different osmolyte solutions (see top legend). We only observe an overshoot when PEO 200k is added; experiments employing only the smaller dextran 70k or PEG 20k do not exhibit an overshoot. The solid lines are fits to our model, with parameters displayed in Table I. (b) The same data plotted in a rescaled fashion to better visualize the relative overshoot.

do observe, after an initially rapid volume increase, a regime where swelling in these solutions occurs much more slowly, at times longer than ≈ 2000 s. This is in agreement with the assumption that smaller osmolytes can penetrate the hydrogel and, as a result, can slowly reduce the external pressure. It thus appears that for these two cases, the reduction of the net external pressure dominates over any possible reduction in effective solvent quality. We therefore hypothesize that for a pronounced overshoot effect to be observed, a mixture of low and high molecular weight osmolytes is required.

To test this hypothesis, we perform measurements where we intentionally add a low molecular weight polymer to the

TABLE I. Fitting parameters for the model curve fits displayed in Fig. 2 to Fig. 4. The upper and lower sections of the table display the swelling and compression cases, respectively. The standard error for each fitted parameter is given in parentheses.

Solution	P (10^{-1})	Γ_α ($10^{-5}/s$)	Γ_f ($10^{-5}/s$)	B (10^{-1})
NaCl only	0	0.94(0.01)		
Dextran 70k 8 wt %	3.3(0.1)	0.75(0.01)	0.10(0.12)	1.9(0.6)
PEG 20k 8 wt %	12.7(0.3)	0.62(0.01)	0.39(0.16)	5.6(0.3)
PEO 200k 2 wt %	0.0(0.8)	1.03(0.02)	2.71(1.20)	5.2(1.2)
PEO 200k 4 wt %	4.0(1.5)	0.88(0.02)	2.69(1.30)	10.3(1.7)
PEO 200k 5 wt %	4.9(2.9)	0.79(0.04)	3.39(1.28)	17.2(2.8)
PEO 200k 7.5 wt %	8.9(5.1)	0.65(0.04)	3.40(1.41)	23.9(3.9)
PEO 200k 10 wt %	19.2(2.6)	0.54(0.01)	1.95(0.50)	30.0(1.6)
PEO 200k 4 wt % + PEG 20k 8 wt %	23.7(1.5)	0.52(0.01)	1.83(0.31)	18.9(0.3)
Dextran 70k 8 wt %	2.8(0.0)	1.96(0.10)	0.44(0.03)	0.9(0.0)
PEG 20k 8 wt %	14.3(0.5)	1.17(0.08)	0.22(0.35)	5.3(2.1)
PEO 200k 4 wt %	1.8(0.1)	5.83(0.78)	7.23(1.27)	12.9(0.2)
PEO 200k 7.5 wt %	2.3(0.2)	9.94(1.45)	5.84(1.12)	16.8(0.3)
PEO 200k 10 wt %	3.4(0.3)	10.90(1.73)	8.16(1.68)	22.0(0.4)

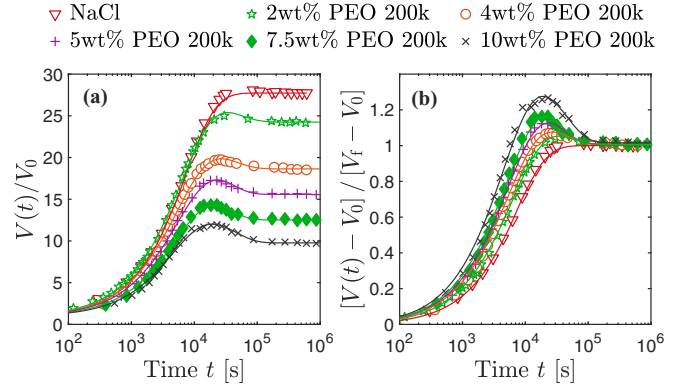


FIG. 3. Swelling in PEO 200k osmolyte solutions of different concentrations. (a) Normalized hydrogel volume $V(t)/V_0$ as a function of time in PEO 200k solutions (for concentrations see top legend). The solid lines are fits to our model, with parameters displayed in Table I. (b) The same data plotted in a rescaled fashion to better visualize the relative overshoot.

PEO 200k solution. Indeed, in experiments where we combine 8 wt % PEG 20k and 4 wt % PEO 200k, shown as filled blue stars in Fig. 2, we observe a more pronounced overshoot than just for PEG 20k or PEO 200k alone at the same concentrations. It thus appears that indeed the combination of low and high molecular weight osmolytes yields a particularly pronounced overshoot. To further study this nonmonotonic swelling behavior, we perform experiments at different concentrations of PEO 200k, shown in Fig. 3. We find that the relative overshoot is more pronounced for higher concentrations of PEO 200k, while it appears that the hydrogels reach their equilibrium volume at approximately the same time, at $t \approx 10^5$ s.

B. Osmotic compression

As a test of the influence of macromolecules on the osmotic compression of hydrogels, we take hydrogel particles that have been swollen in a saline solution for at least a week. We then place these particles in solutions containing the small PEG 20k or dextran 70k, as well as the larger PEO 200k. We perform these osmotic compression experiments at concentrations of 8 wt % PEG 20k, 8 wt % dextran 70k, and 4, 7.5, and 10 wt % of PEO 200k, respectively. Indeed, when using the smaller PEG 20k and dextran 70k we do observe a pronounced reswelling, as depicted in Fig. 4, a clear indication that a penetration of these small macromolecules into the hydrogel is occurring. We note that for both osmolytes the reswelling starts at around the same time ($\pm 10^4$ sec), indicating that the penetration of both polymers occurs at approximately the same rate. This is reasonable, as the two polymers have similar molecular weights and we would therefore expect their diffusion coefficients within the network to be similar. In corresponding *swelling* experiments, performed at the same concentrations, we observe a transition from fast to slow swelling after a similar period of time, as shown in Fig. 2. For the PEO 200k solutions we observe no reswelling, indicating that—in analogy to the swelling experiments—the low molecular weight osmolyte penetrates into the hydrogel,

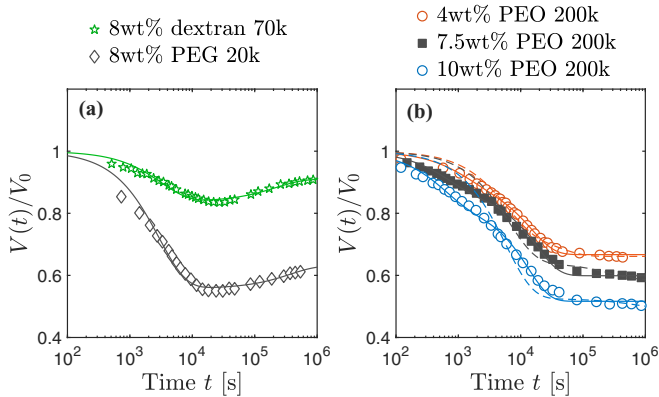


FIG. 4. Osmotic compression in osmolyte solutions of different molecular weight. Normalized volume $V(t)/V_0$ as a function of time. (a) In the low molecular weight osmolytes dextran 70k and PEG 20k, a slow reswelling after an initially fast compression is observed. (b) In high molecular weight PEO 200k solutions, an initially fast compression is followed by a regime of further, albeit slower compression. For osmolyte parameters see top legend. The solid lines are fits to our model, with parameters displayed in Table I. The dashed lines are fits where Γ_α is fixed to the value obtained from the corresponding swelling experiments, with parameters displayed in Table III.

thereby lowering the effective solvent quality. We also observe an additional deswelling process at longer timescales, which again hints at the polydispersity of the used PEO 200k, and the resultant slow penetration of a high molecular weight fraction of osmolyte into the network.

Our experiments thus illustrate that, in order to perform an osmotic compression experiment that is straightforward to analyze, it is important to use as osmolytes macromolecules that are sufficiently large and sufficiently monodisperse. This is because otherwise a fraction of the osmolyte would be able to enter the particle. Any osmolyte fraction that enters the gel network changes the osmotic pressure inside the gel, either directly, by its mere presence, or indirectly, by changing the effective solvent quality.

C. Model

To account for the observed behavior, we develop, based on the simple phenomenological model from our previous study [13], an extended model, which incorporates the modification of the effective solvent quality, brought about by the presence of macromolecules within the network of the hydrogel particles, as well as, related to this, a potentially uneven equilibrium distribution of these osmolyte macromolecules between the inside and the outside of the hydrogel, implying a remaining osmotic pressure difference.

We assume that if a particle is subjected to a pressure difference by immersing it in a polymer solution, this jump is instantaneous and that the pressure depends on the concentration of the osmolyte. We consider three separate regimes for the size of the osmolyte compared to the pores of the network:

The first regime is where the radius of gyration R_g of the osmolyte polymer chain is much larger than the network's mesh size ζ , $R_g \gg \zeta$. In this limit, we assume that the osmolyte

does not penetrate the hydrogel network within experimental timescales.

The second regime is when the polymer chains are much smaller than the network's mesh size, $R_g \ll \zeta$, in which case the diffusion of the molecules inside the network is nearly unhindered.

Describing the third regime between these two limiting cases, $R_g \sim \zeta$, is not trivial. In our model we directly employ the diffusion coefficient of the osmolyte within the network D_{osm} to describe the mobility of the polymer chains within the network. While this diffusion coefficient depends on the molecular weight of the polymer and the mesh size of the network, a theoretical prediction based on these parameters is not straightforward [27,28]. Due to the presence of the network, we assume that the diffusion of the osmolyte inside the particle is slower than diffusion of the osmolyte outside the particle. And because diffusion of osmolyte into the hydrogel is slow, the hydrogel particle responds elastically to the osmotic pressure difference caused by different concentrations of osmolyte inside and outside the gel particle. Therefore, we assume that initial volume changes are dominated by elastic effects.

At $t = 0$ the osmolyte concentration inside the particle is 0 and the outside osmolyte concentration stays fixed during the experiment. Our simple model does not specifically take into account the spatial distribution of the osmolyte within the particle, instead regarding only the time dependent average osmolyte concentration within the entire particle. In our previous experiments [13], we flow fresh background fluid past the particle, thereby ensuring that the outside concentration remains constant and homogeneous. To the same end, in our current experiments we submerge the macroscopic hydrogel particles in a large container of background fluid under constant stirring of the fluid on a roller bank. A large volume of the fluid reservoir ensures that any osmolyte absorption into the hydrogel does not significantly affect the outside concentration. As our background fluid has roughly 50 times more volume than the hydrogel particle in its swollen state, this is a reasonable assumption. As we actively stir the solutions we also assume that the concentration of osmolyte outside the particle, and near the particle surface, is homogeneous.

Similarly to what we did in our previous study [13], we assume model A dynamics [29] for the volumetric response of a hydrogel particle, which provides a governing equation for the radius of the particle $\dot{R} = -\Gamma \partial \Psi / \partial R$, where Γ is a phenomenological rate constant and Ψ is the free energy of the hydrogel. The free energy is given as

$$\Psi = \overbrace{m \frac{3}{2} k_B T \left(\frac{R}{R_0} \right)^2}^{\text{elasticity}} + m \frac{3}{2} k_B T \left(\frac{R_0}{R} \right)^2 + \underbrace{N k_B T (\log \rho v - 1)}_{\text{mixing}} - \underbrace{\frac{N \mu}{\text{uptake}} + \Pi \frac{4\pi R^3}{3}}_{\text{expansion}} - \underbrace{k_B T B m \frac{\rho}{\rho_w}}_{\text{interaction}}, \quad (1)$$

where the first two terms account for elastic deformations relative to the osmolyte-free equilibrium state at radius R_0 . The third term measures the mixing free energy of the osmolyte in the particle, the fourth quantifies the energetic cost of taking

up osmolyte molecules from the surrounding solution, and the fifth measures the cost of hydrogel expansion in the solution. The last term, parametrized by B , is an interaction term with the role of a (cross) virial coefficient which can be positive or negative, depending on the interactions between the solvent, osmolyte, and polymer network. We define m as the number of crosslinked subchains, N is the number of osmolyte molecules in the hydrogel particle, $\rho \equiv 3N/4\pi R^3$ is the mean density of osmolyte inside the particle, v is a microscopic volume scale, and μ and Π are, respectively, the chemical potential and osmotic pressure of the osmolyte in the surrounding solution.

If the background fluid behaves like an ideal solution, we can apply van 't Hoff's law to the osmotic pressure $\Pi = k_B T \rho_w$ of the outside solution, with ρ_w the mean density of osmolyte. Due to hydrogel-osmolyte interactions the osmolyte concentration inside and outside the particle are not necessarily equal in the final equilibrium state, but are characterized by the equilibrium partition coefficient Q [27], as

$$Q \equiv \frac{3N_{\text{eq}}/4\pi R_{\text{eq}}^3}{\rho_w}, \quad (2)$$

where N_{eq} and R_{eq} are, respectively, the number of osmolyte molecules inside the particle, and the particle radius in the final equilibrium state. The equilibrium partition coefficient measures the resulting ratio of osmolyte concentrations inside and outside of the hydrogel particle. In case the osmolyte molecules are point particles, i.e., their radius of gyration R_g is much smaller than the mesh size of the hydrogel network ζ , and if they experience no long-range interactions with the hydrogel, Q equals the volume fraction of solvent $\phi \equiv 1 - (R_{\text{dry}}/R_{\text{eq}})^3$, with R_{dry} the radius of a dry hydrogel network. We estimate Q as the fraction of available volume in the particle for a specific osmolyte, therefore all solvent-quality related interactions are absorbed in B . Thus, for osmolyte molecules of nonzero size able to penetrate the hydrogel particle, $0 < Q < \phi$.

In principle, for a full description of the hydrogel-osmolyte-solvent interactions, we would require three Flory-Huggins-type [30,31] parameters to quantify the impact of the solvent quality for both the network and osmolyte, and the interaction between network and osmolyte [32]. For simplicity, we choose a description using only the effective energetic parameter B .

Definition of the normalized particle radius as $\alpha(t) \equiv R(t)/R_0$ leads to a modified evolution equation for the particle radius

$$\frac{\partial \alpha}{\partial t} = -3\Gamma_\alpha \left[\alpha - \frac{1}{\alpha^3} - P \left(\frac{fQ\alpha_{\text{eq}}^3}{\alpha} - \alpha^2 \right) + B \frac{fQ\alpha_{\text{eq}}^3}{\alpha^4} \right], \quad (3)$$

where $P \equiv \Pi/K$ is the osmotic pressure, scaled by the bulk compressive modulus $K \approx 3k_B T m/4\pi R_0^3$ of the network, and $\Gamma_\alpha \equiv m\Gamma k_B T/R_0^2$ is a relaxation rate. We defined $\alpha_{\text{eq}} \equiv R_{\text{eq}}/R_0$ as the ratio of the particle radius in the final equilibrium state R_{eq} to that in the osmolyte-free state R_0 , and we define $f(t) = N(t)/N_{\text{eq}}$ as the amount of osmolyte in the hydrogel particle at time t relative to that in the final state, N_{eq} .

To account for diffusion of the osmolyte from the fluid into the hydrogel particle, we use the diffusion equation in

integral form, $\partial N/\partial t = D_{\text{osm}} \oint d^2S \cdot [\rho \nabla \mu/k_B T]$ across the interface, where D_{osm} is the diffusivity of the osmolyte within the gel. We treat the concentrations inside and outside the hydrogel particle as uniform but different. This becomes $\partial N/\partial t = CD_{\text{osm}}R^{-2}(N_{\text{eq}} - N)$ with $R(t)$ the radius of the hydrogel particle and N_{eq} the number of osmolyte particles in the final equilibrium state; C is a proportionality constant to be determined by comparison with the known solution of the diffusion equation for osmolytes diffusing through a static hydrogel network (see Sec. III E). In normalized form, the diffusion equation reads

$$\partial f/\partial t = -\Gamma_f \alpha^{-2}(f - 1), \quad (4)$$

with $\Gamma_f \equiv CD_{\text{osm}}/R_0^2$ the kinetic parameter that sets the timescale for the solute to enter the hydrogel particle by diffusion. The final equilibrium radius R_{eq} can be found from Eqs. (3) and (4) in the static limit.

If the osmolyte cannot penetrate into the hydrogel, $Q = 0$ and the particle will simply compress or swell monotonically under influence of the applied constant pressure; see the right column in Fig. 5. For $B = 0$ the osmolyte does not alter the effective solvent quality for the hydrogel network, and the final volume is determined by the osmotic pressure difference between the inside and the outside of the particle; see the top row in Fig. 5. By ignoring long-range interactions and regarding the hydrogel network as a phantom network, i.e., $B = 0$ and $Q = \phi \approx 1$, the model reduces to the version we described in Sleeboom *et al.* [13]; see the top left scenario in Fig. 5. In this case, the osmolyte can penetrate the network and does not interact with it in any way; as a consequence, in the final equilibrium state the concentrations inside and outside the hydrogel particle are the same.

For $B \neq 0$ and $Q > 0$ the osmolyte penetrates the gel and the effective solvent quality is affected by the presence of the osmolyte. This generally results in a modification of the final volume, except in the special case where the osmotic pressure difference between the inside and the outside of the particle balances the effect of increased effective solvent quality, i.e., $BQ - P(Q - 1) \approx 0$. Using this relation, we reanalyze the experiments of Sleeboom *et al.* [13] in Appendix F. For the experiments in the present study, the illustrations in the middle column at the middle row of Fig. 5 summarize the different qualitative behaviors for both swelling and compression experiments.

D. Fitting results

By fitting this extended model to the experimental data we can obtain the permeability κ , the compressive modulus K , and the diffusivity of the osmolyte in the hydrogel D_{osm} , and in our modified version, we also obtain an indication for the effective solvent quality of the osmolyte in the form of the parameter B . We fit our model to our experiments using the Mathematica functions ‘‘NonlinearModelFit’’ and ‘‘NDSolve’’ where we set P , Γ_α , Γ_f , and B as fitting parameters. We estimate Q as the fraction of available volume for the different osmolytes in the hydrogel particle. For dextran 70k, PEG 20k, and PEO 200k, we find $Q^{\text{dex}} = 0.78$, $Q^{\text{PEG}} = 0.75$, and $Q^{\text{PEO}} = 0.36$, respectively; see Appendix F. The results of this fitting procedure are shown in Fig. 2 to Fig. 4.

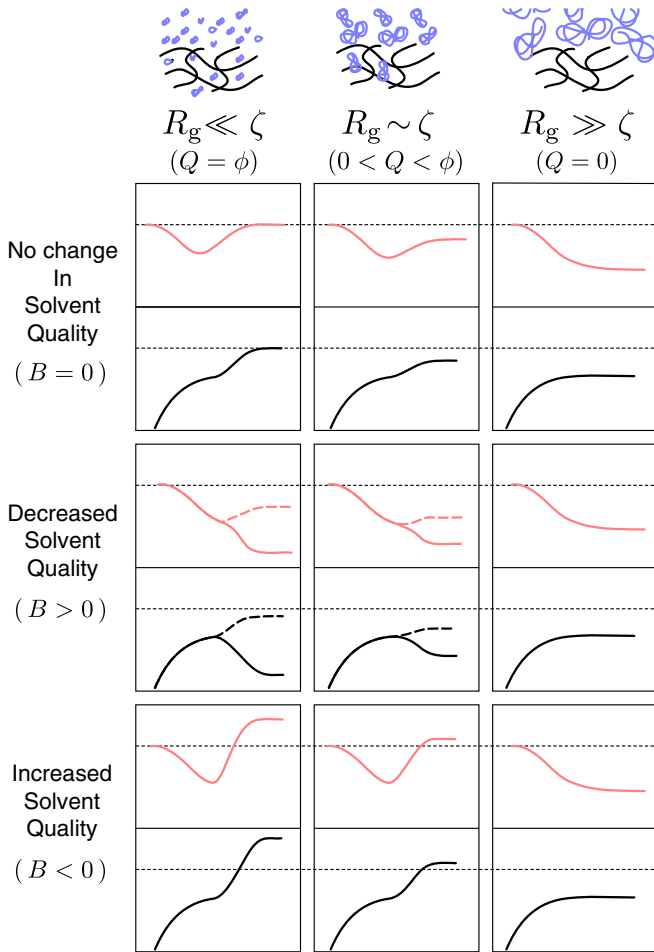


FIG. 5. Schematic illustration of the different theoretical scenarios for the time evolution of the volume of a hydrogel particle on a log-linear scale under compression (solid red lines) and swelling (solid black lines) in polymer solutions, as a function of both the ratio of the radius of gyration R_g of the dissolved macromolecules to the mesh size of the hydrogel network ζ (columns) and their effect on the effective solvent quality of the solution B with respect to the hydrogel network (rows). The horizontal dotted lines indicate the osmolyte-free equilibrium level of swelling of the hydrogel particle. If $R_g \ll \zeta$ or $R_g \sim \zeta$, osmolyte can diffuse into the hydrogel particle (left and middle column). When there is no change in effective solvent quality (top row), the difference in osmotic pressure between the inside and the outside of the particle decreases over time due to osmolyte diffusion, causing slow (additional) swelling. A small decrease in effective solvent quality (middle row, dotted curve) can cause an undershoot in a compression experiment, whereas a large decrease in effective solvent quality (middle row, solid curve) can cause an overshoot in a swelling experiment. Increases in effective solvent quality (bottom row) enhance the magnitude of slow (re)swelling.

We have summarized the parameters obtained from the fitting procedure in Table I. We first analyze the parameters obtained for the hydrogels swollen in PEO 200k to verify that the parameters are consistent. For these hydrogels we observe an increase in P for increasing polymer concentrations, which is as expected, as the external pressure, $P \propto \Pi$, increases with increasing polymer concentration. We expect that the decay rate for the particle radius Γ_α decreases with increasing

polymer concentration, because a higher network polymer density in the particle lowers the permeability for solvent molecules, and indeed, we do observe a slight decrease in Γ_α for increasing polymer concentration. We also observe a trend for an increase of Γ_f with increasing PEO 200k concentration, which is somewhat expected, as the mutual diffusion coefficient increases with polymer concentration [33]. Further, we observe an increase of the parameter B with increasing PEO 200k concentrations. This is reasonable, as the interaction term in Eq. (3) is not proportional to the absolute concentration of solute, and therefore the effect of increasing polymer concentration shows itself in B . The P values for the hydrogels swollen in PEG 20k 8 wt % and dextran 70k 8 wt % are also consistent, as the PEG 20k solution has a much higher osmotic pressure than the dextran 70k solution, 65(9) kPa [34] versus 10 kPa [23], respectively, where the estimated uncertainty, if available, is displayed in parentheses.

For the compression experiments all the obtained values for dextran 70k and PEG 20k are comparable to those from the swelling experiments. For PEO 200k the obtained values for P and B in the compression experiments exhibit the same trends as those observed in the swelling experiments.

However, we find significant differences between the values of Γ_α and Γ_f obtained from the compression and the swelling experiments, respectively. While the rate of change of the particle radius to its equilibrium value R_{eq} is set by Γ_α , the rate constant Γ_f sets the timescale for osmolyte diffusion, which may induce slow (de)swelling of the hydrogel particle by changing both the effective solvent quality and the osmotic pressure difference; see Fig. 5 for an illustration. Therefore, if the measured volume does experience an under- or overshoot, as observed for the dextran 70k and PEG 20k compression experiments in Fig. 4(a), the undershoot can be taken into account uniquely by the slow diffusion of osmolyte, thereby determining Γ_f . However, the PEO 200k compression experiments in Fig. 4(b) exhibit no undershoot, thus making the effects contained in Γ_α and Γ_f less clearly separated and their values prone to error.

E. Material properties

We can relate the model parameters to the bulk modulus K , the permeability κ , and the diffusion coefficient of the osmolyte in the network D_{osm} . We determine K directly from the fitted P value as we defined $P = \Pi/K$. From literature we know Π as a function of concentration, for both the dextran 70k [23] and the PEG 20k [34] solutions used in our experiments, but not for our PEO 200k solutions. To determine Π as a function of concentration for our PEO 200k solutions, we place 1 mL samples of a 2 wt % PEO 200k solution in dialysis bags and submerge them in dextran solutions of various concentrations with known osmotic pressures. After having given the samples a week to equilibrate, we extract the PEO 200k concentration as a function of osmotic pressure, assuming that the osmotic pressure inside has equilibrated to the pressure outside; see Appendix B for details.

To determine the permeability κ , we consider the (hypothetical) case of the swelling of an initially compressed hydrogel without osmolyte and find from Eq. (3) an exponential long-time relaxation at a rate of $12\Gamma_\alpha$. Assuming that

TABLE II. Material properties based on the model fits displayed in Fig. 2 to Fig. 4. The upper and lower sections of the table display the swelling and compression cases, respectively. The standard error for each material parameter is given in parentheses. We assume all fitted parameters to be uncorrelated.

Solution	Π (kPa)	K (kPa)	κ (nm ²)	D_{osm} ($\mu\text{m}^2/\text{s}$)
NaCl only	0	27	5.7(0.1)	
Dextran 70k 8 wt %	10.4	32(1)	3.9(0.1)	1.3(1.6)
PEG 20k 8 wt %	64.7(8.6)	51(7)	2.0(0.3)	5.3(2.2)
PEO 200k 2 wt %	0.4(0.3)	633(73800)	0.3(31.0)	37.0(16.4)
PEO 200k 4 wt %	6.1(0.6)	15(6)	9.6(3.7)	36.7(17.8)
PEO 200k 5 wt %	10.8(0.8)	22(13)	5.8(3.5)	46.3(17.5)
PEO 200k 7.5 wt %	28.4(1.4)	32(18)	3.3(1.9)	46.4(19.3)
PEO 200k 10 wt %	54.1(2.2)	28(4)	3.2(0.5)	26.6(6.8)
PEO 200k 4 wt % + PEG 20k 8 wt %	70.7(8.6)	30(4)	2.9(0.4)	25.0(4.3)
Dextran 70k 8 wt % + PEG 20k 8 wt %	10.4	37(1)	8.7(0.4)	6.0(0.4)
PEG 20k 8 wt % + PEO 200k 4 wt %	64.7(8.6)	45(6)	4.2(0.7)	3.0(4.7)
PEO 200k 4 wt % + PEO 200k 7.5 wt %	6.1(0.6)	33(4)	28.9(5.1)	98.7(17.4)
PEO 200k 7.5 wt % + PEO 200k 10 wt %	28.4(1.4)	124(11)	13.1(2.2)	79.7(15.3)
PEO 200k 10 wt %	54.1(2.2)	161(15)	11.0(2.0)	112.0(23.0)

this rate corresponds to the dominant relaxation rate in the long-time limit of the analytical swelling model of Tanaka and Fillmore [6], we obtain $12\Gamma_\alpha = \pi^2 K \kappa / R_0^2 \eta$, with η the viscosity of water. This expression is an improvement on the one of our previous work [13], where we compared the short-time swelling response of our phenomenological model to the long-time response of the analytical swelling model of Tanaka and Fillmore.

Finally, we can estimate D_{osm} from the rate constant Γ_f . To do so, we need to realize that in our phenomenological model we had absorbed the unknown prefactor C in the definition of Γ_f . To determine C , let us consider the (hypothetical) case where the particle radius remains fixed, $\Gamma_\alpha = 0$, but diffusion of osmolyte can still occur. In this case, the only relevant process is the diffusion of osmolyte into the network, and we can solve Eq. (4) for all times, which yields Γ_f as an exponential relaxation rate. Setting this rate equal to the dominant relaxation rate in the long-time limit of the analytical solution of the diffusion equation in a sphere of radius R_0 [35], we obtain $C = \pi^2$. This determination of C is an improvement to our previous work [13], where we had put $C = 1$.

We have placed all of these results in Table II. From the swelling experiments (upper section of the table) we obtain an average value of 35(9) kPa for K and 4(2) nm² for κ . We obtained these averages by weighting each value with the inverse square of its standard error; the corresponding standard deviation is displayed in parentheses. These parameters are in fair agreement with the values of $K = 27(6)$ kPa and $\kappa = 8(5)$ nm², obtained in separate, conventional experiments. To obtain these experimental values for K and κ , we used a macroscopic version of the capillary micromechanics technique [36] and a custom-built permeability measurement setup, respectively (see Appendix C and Appendix D).

We notice that the osmolyte diffusion coefficient D_{osm} obtained from the swelling experiments for the dextran 70k and

TABLE III. Model parameters and material properties obtained by fitting P , Γ_f , and B for the PEO 200k compression experiments, using Γ_α from the corresponding swelling experiments shown in Table I.

	4 wt %	7.5 wt %	10 wt %
P	5.9(0.2)	9.4(0.5)	16.9(1.1)
Γ_α	0.88	0.65	0.54
Γ_f	2.21(0.83)	0.29(0.08)	0.10(0.76)
B	8.5(0.5)	10.4(1.4)	12.3(14.8)
Π	6.1(0.6)	28.4(1.4)	54.1(2.2)
K	10(1)	30(2)	32(2)
κ	14.1(1.4)	3.5(0.2)	2.8(0.2)
D_{osm}	30.2(11.3)	3.9(1.1)	1.4(10.3)

the PEG 20k solutions is consistently lower than for the PEO 200k solution. The reason for this could be that, while overall the PEO 200k has a higher molecular weight than PEG 20k and dextran 70k, the fraction of the polydisperse PEO 200k species that is small enough to penetrate the hydrogel could still diffuse faster than the dextran 70k or PEG 20k polymers. Indeed, in experiments employing a mixture of PEG 20k and PEO 200k we obtain a diffusion coefficient D_{osm} that lies between those observed for PEO 200k and for PEG 20k.

The anomalously high values for K , κ , and especially D_{osm} obtained from the PEO 200k compression experiments are possibly caused by the monotonic decrease of hydrogel volume in these compression experiments, which makes the effects of osmolyte diffusion (Γ_f) and the rate of solvent permeation of the hydrogel particle (Γ_α) difficult to distinguish; see Sec. III D for more information. Indeed, if we fix Γ_α with the value fitted from the corresponding swelling experiment, we find values for K , κ , as well as D_{osm} that are closer to those of PEG 20k and dextran 70k; see Table III. The corresponding fit curves are displayed in Fig. 4 as dashed lines.

Overall, given the simplicity of our model, for the swelling experiments the model accounts for the experiments surprisingly well, even as we neglected any polydispersity effects. Nevertheless, it could be useful to develop an improved model that specifically accounts for this factor. In our phenomenological model we also neglected any possible blocking or slowdown of shorter chains by a potential buildup of longer chains near the surface of the swelling hydrogel. We would indeed expect such a buildup to occur, as a simple estimation (see Appendix E) predicts that during swelling the particle surface advances into the background liquid faster than the PEO 200k can diffuse away. This would lead to the formation of a dense layer of high molecular weight polymer chains near the surface, which would delay the penetration of shorter chains into the hydrogel particle. Such a hypothesized delay of the osmolyte entering the network is not specifically considered in our model. We would expect its effects to manifest themselves in our model, however, in the form of a lowered diffusion coefficient of the osmolyte within the network.

From the results of Table I we conclude that the decrease in effective solvent quality is stronger for PEO 200k than for both dextran 70k and PEG 20k. This is a key

ingredient needed to explain the long-time hydrogel particle dynamics in every swelling and compression experiment we conducted. In the experiments (part of) the osmolyte slowly diffuses into the hydrogel, as witnessed by the (de)swelling and (de)compression processes happening on long timescales in Figs. 1–4. By diffusing into the hydrogel, the osmolyte lowers the osmotic pressure difference, thereby inducing swelling of the hydrogel, lowering the effective solvent quality at the same time. This causes compression of the hydrogel. The competition between these two effects determines the measured volumetric response of the hydrogel particle at long timescales; see Fig. 5 for an illustration. For the dextran 70k and PEG 20k the decrease in osmotic pressure difference prevails, causing additional slow swelling in the swelling experiments and slow decompression in the compression experiments; see Figs. 2(a) and 4(a). On the other hand, for PEO 200k the decrease in effective solvent quality prevails, causing slow compression in the swelling experiments, which results in the observed overshoot; see Fig. 3. Also, it causes additional slow compression in the compression experiments; see Fig. 4(b).

For dextran 70k and PEG 20k the diffusion constant in the swelling and compression experiments is consistent and reflects their monodispersity. However, from fits to the data for PEO 200k, after fixing the swelling timescale Γ_s , we obtain significantly higher diffusion coefficients from the swelling experiments than from the corresponding compression experiments (see Tables II and III). Due to the broad size distribution of PEO 200k, the fraction of small PEO molecules, which are of approximately the size of dextran 70k and PEG 20k, are the first to diffuse into the hydrogel. Therefore, the small fraction is the first to decrease the effective solvent quality and induce compression of the hydrogel particle. As this compression shows itself as a pronounced overshoot in the hydrogel volume on which we fit our model, we obtain the diffusion constant of the fraction of small PEO molecules from the swelling experiments. We hypothesize that this apparent diffusion constant is enhanced due to the fast increase in hydrogel radius; see Appendix E. As a result, the swelling hydrogel imbibes the solvent as well as small PEO molecules. Therefore, we find a relatively large apparent diffusion constant in the swelling experiments albeit with a large uncertainty due to the additional compression caused by the fraction of larger PEO molecules; see Table II. In the PEO 200k compression experiments, however, the compression caused by changes in effective solvent quality, induced by the low- M_w fraction of PEO 200k, coincides with a compression purely due to osmotic pressure differences. As soon as the osmotic pressure difference is balanced by the elasticity of the hydrogel network, the additional slow compression is fully determined by the high- M_w fraction of PEO 200k molecules diffusing into the hydrogel particle, implying a much lower diffusion coefficient; see Table III.

IV. CONCLUSIONS

We have performed swelling and compression experiments with hydrogels in solvents containing macromolecules that, depending on their size, can, to different degrees and at different rates, penetrate the hydrogel network. Our experiments

show that when such macromolecules penetrate a hydrogel network, significant changes in effective solvent quality can occur, which directly affect the equilibrium swelling volume as well as the transient swelling and deswelling dynamics.

During swelling experiments in the presence of a slowly penetrating osmolyte we find a stretched-out swelling behavior. We further observe that when a combination of large and small osmolytes is used, an overshoot in the swelling can occur. In our physical picture of this effect, the small osmolyte penetrates the hydrogel and thereby lowers the effective solvent quality, while also contributing to a reduction in the osmotic pressure difference.

By the same argument, during a compression experiment, after the initial compression, the penetration of osmolyte macromolecules leads to a further compression or reswelling to a final size that depends on the change in effective solvent quality brought about by the presence of osmolyte macromolecules within the network.

Thus, a meaningful description and understanding of the swelling and compression of hydrogels in polymer solutions has to specifically take polymer-induced changes of the effective solvent quality into account. To do so, we have developed a simple phenomenological model that accounts for both the swelling and the compression of hydrogels in the presence of macromolecules dissolved in the background liquid. The model takes into account both the reduction of the osmotic pressure difference and the changes in effective solvent quality that are induced by the penetration of macromolecules into the gel network.

Despite its simplicity, our model accounts for the qualitative behavior that is observed when swelling (or compression) of a hydrogel network occurs in the presence of macromolecules within an aqueous background liquid. Moreover, even quantitatively, we find good agreement with swelling and compression experiments performed under a variety of conditions with different sizes and types of macromolecules dissolved in the background saline solution. Fitting our data to the phenomenological model enables us to estimate the compressive modulus, the network permeability, the diffusivity of the osmolyte inside the hydrogel, as well as to give an indication for the changes in effective solvent quality in the presence of osmolyte macromolecules.

We expect this work to be relevant to all fields of research and applications that involve the swelling of porous hydrogel materials in the presence of macromolecules and other solutes, as well as for applications where osmotic compression experiments are used for determining the mechanical properties of soft, porous objects.

ACKNOWLEDGMENTS

The work of F.J.A. and H.M.W. forms part of the research program of the Dutch Polymer Institute (DPI), Project No. 738; we are grateful for its financial support. The work of M.T.J.J.M.P. is part of the Industrial Partnership Programme Hybrid Soft Materials that is carried out under an agreement between Unilever R&D B.V. and the Netherlands Organisation for Scientific Research (NWO).

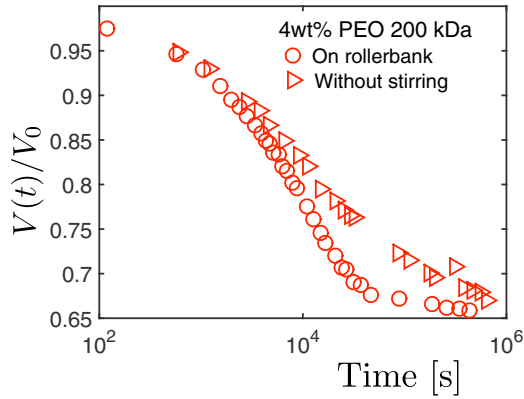


FIG. 6. Normalized weight as a function of time for a sample on and off the roller bank.

APPENDIX A: ROLLER BANK

We measure the weight of a hydrogel particle, which has been swollen in a saline solution for at least a week, as a function of time, after we submerge it in a PEO solution (see Fig. 6). For samples exposed to an osmotic shock at rest, without using the roller bank, a distinct delay in compression is observed. We hypothesize that this has to do with the formation of a depletion zone around the particle, as the surface of the hydrogel retracts faster than the PEO can follow by diffusion; see Appendix E. Changing the settings of the roller bank might also influence this process, but we have not investigated this in detail.

APPENDIX B: OSMOTIC PRESSURE PEO

We measure the osmotic pressure of the PEO solutions as a function of concentration by dialysis against dextran solutions, for which the osmotic pressure has previously been measured in detail [23]. We enclose 2 wt % PEO solutions into dialysis bags and place them into baths of dextran solutions of various concentrations with corresponding osmotic pressures ranging from 0.9 kPa to 40.7 kPa. These baths are then allowed to equilibrate for a period of 1 week. After this period we assume that the osmotic pressure of PEO inside the bag matches that of dextran in the bath outside. Depending on whether the initial osmotic pressure in the PEO solution is larger or smaller than that in the surrounding dextran solution, the concentration within the dialysis bag will have increased or decreased after equilibration, respectively. We neglect changes in concentration in the dextran bath around the dialysis bag, as the volume of the dextran solution far exceeds the volume of the sample in the dialysis bag (ratio 50:1).

To determine the concentrations of the equilibrated PEO solutions, we extract the solutions from the dialysis bags and determine their weight both immediately after extraction and after thorough overnight drying on a hot plate, respectively. The PEO weight concentration is then taken as the ratio of the dry weight to the initial weight of the solution. The resulting data points for the different solutions are shown in Fig. 7 as blue circles. The red line is a second-order polynomial fit to the data, which adequately describes the experimental

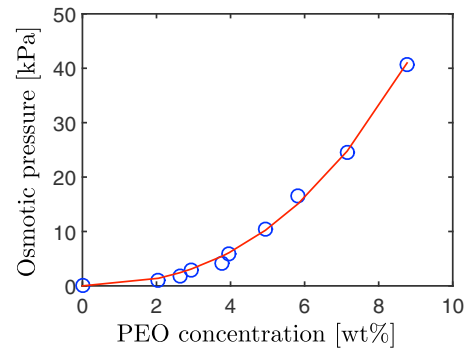


FIG. 7. Osmotic pressure as a function of concentration for PEO solutions, as determined from dialysis against dextran solutions. The blue circles are the experimental data, and the red line is our second-order polynomial fit.

data over the range of concentrations studied. To obtain the osmotic pressure of PEG 20k from literature [34], we also used a second-order fit of the measured osmotic pressure in the range of 0–10 wt %.

APPENDIX C: CAPILLARY MICROMECHANICS

As a comparison with our osmotic compression experiments, we quantify the mechanical properties of our hydrogel particles using the recently developed capillary micromechanics method [36]. The results serve as a validation for our developed model. During capillary micromechanics, a particle of interest is flown into a tapered glass capillary of circular cross section. As the tip of the capillary is smaller in diameter than the particles, the particle gets trapped and subsequently blocks the flow. In this situation, the entire pressure difference applied across the capillary falls off across the trapped particle. The corresponding applied external stress must match the internal elastic stress within the particle, which is a function of the particle's deformation and the elastic moduli of the particle. As the particle changes both its shape as well as its volume in the process, quantifying its deformation enables us to directly extract the full elastic response, including the compressive (bulk) modulus K and the shear elastic modulus G . To extract K , we quantify the volumetric strain $\Delta V/V$ as a function of the characteristic bulk stress $\sigma_{\text{compr}} \approx (2p_{\text{wall}} + p)/3$ applied to the particle, where p_{wall} is the pressure exerted on the particle at the area of contact between the particle and the wall of the capillary, and p is the pressure drop applied across the capillary. The result for a particle which is swollen in a saline solution for at least a week is depicted in Fig. 8. From the slope we find $K = 27(5)$ kPa, with the fit uncertainty in parentheses.

APPENDIX D: HOMEBUILT PERMEABILITY SETUP

The permeability κ is measured using a homebuilt setup consisting of a thin-walled glass capillary (TW120-6, WPI, USA) and a pressure regulator (MFC-EZ, Fluigent, Germany). In the capillary we create an hourglass-shaped notch by controlled pulling with a micropipette puller (model P-97, Sutter Instruments, USA). The function of this notch is to prevent the hydrogel from moving forward when pressure is

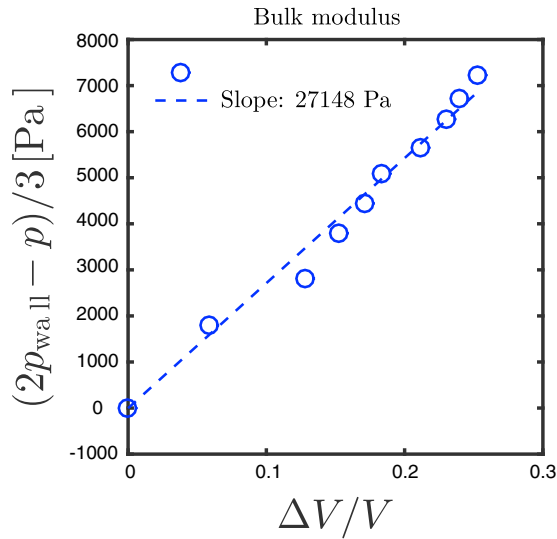


FIG. 8. Volume change $\Delta V/V$ as a function of the characteristic bulk stress $(2p_{\text{wall}} + p)/3$, as measured using capillary micromechanics.

applied to it. To prevent air bubbles in the system, we first fill the capillary with the solvent in which the hydrogel of interest has been swollen. Hereafter we insert the hydrogel by piercing the capillary through the hydrogel, thereby cutting out a cylindrical piece of hydrogel that fits snugly into the capillary. Finally we connect the pressure setup to the capillary. We apply pressures between 0.8 kPa and 4 kPa and track the movement of the solvent-air interface as a function of time after the application of pressure. A schematic overview of the setup is shown in Fig. 9. According to Darcy's law, the flow velocity is proportional to the pressure drop ΔP , as $u\eta L = \Delta P\kappa$, with u the fluid flow rate, η the viscosity, and L the length of the porous material over which the pressure difference is applied. To obtain the permeability κ , we thus plot the scaled flow rate ($u\eta L$) as a function of the pressure difference ΔP , as shown in Fig. 10; the permeability can be directly extracted as the slope of the resultant curve. We have plotted the results for two particles. We here obtain permeabilities of $\kappa = 8(5) \text{ nm}^2$, with the uncertainty in parentheses. These values are reasonable and within the range of permeabilities previously reported for hydrogels of similar polymer concentration.

APPENDIX E: SURFACE MOVEMENT

During swelling, the outer surface of the hydrogel particle is moving through the background liquid at a significant velocity. It is reasonable to assume that high-molecular weight polymers, which cannot readily enter into the network, may accumulate near the advancing interface as a result. This

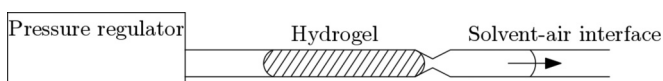


FIG. 9. Homebuilt setup to determine the permeability of hydrogel particles.

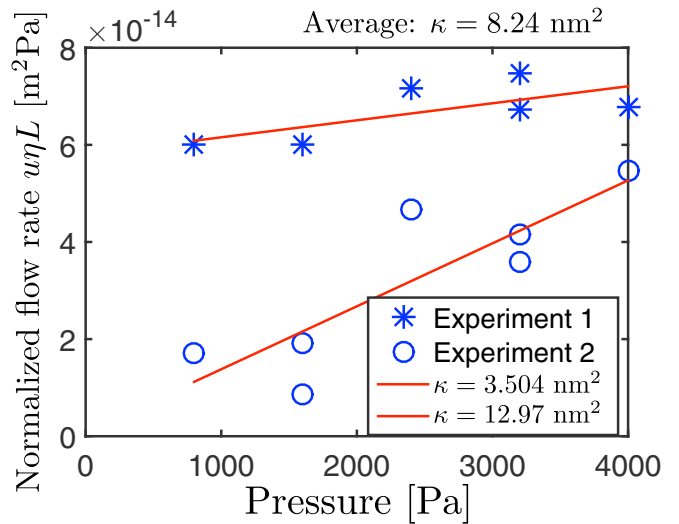


FIG. 10. Normalized flow rate as a function of applied pressure. The slope indicates the permeability.

would be expected to happen if the typical rate at which the polymer chains move away from the surface by diffusion is much slower than the rate at which the hydrogel surface propagates into the solution. To estimate the relative importance of these two effects, we calculate the speed of the surface v_{swell} as \dot{V}/A , with \dot{V} the time derivative of the particle volume and $A(t)$ the corresponding particle surface area. We obtain \dot{V} by fitting the $V(t)$ data with a double exponential form and calculating the time derivative of this fit function. As a characteristic diffusion velocity v_{osmolyte} of the dissolved macromolecules at a length scales comparable to the macromolecule's size, we calculate a typical velocity by calculating the typical diffusion timescale τ_D for a polymer coil to diffuse in one direction over its own radius, for which we have $R_g^2 = 2D\tau_D = \frac{k_B T}{3\pi\eta R_g} \tau_D$, yielding $v_{\text{osmolyte}} = R_g/\tau_D = k_B T/3\pi\eta R_g^2$. The ratio between these two velocities indicates whether we expect the polymer to accumulate near the particle surface (for $v_{\text{swell}}/v_{\text{osmolyte}} \gg 1$) or to disperse by diffusion, unaffected by the swelling process (for $v_{\text{swell}}/v_{\text{osmolyte}} \ll 1$). Indeed, as shown in Fig. 11, the velocity ratio $v_{\text{swell}}/v_{\text{osmolyte}}$ is much larger than unity during almost the entire swelling process. Based on this simple estimation we would thus expect the macromolecules to accumulate near the interface. We do not observe clear evidence of this in our experiments, however.

We perform the same type of analysis for the particles that are being *compressed*. We fit the compression data with a double exponential and determine the time derivative based on the results. We then compare this speed with the diffusion velocity. As depicted in Fig. 12 also during compression the surface moves faster than the osmolyte. In contrast to the swelling case, here this will lead to the formation of an exclusion zone near the particle surface, which effectively lowers the applied osmotic pressure on the particle, slowing down the compression. Indeed, the occurrence of such a slowdown is observed in a compression experiment without external mixing, as compared to an experiment where the external polymer solution is continuously mixed by a roller bank, as shown in Appendix A.

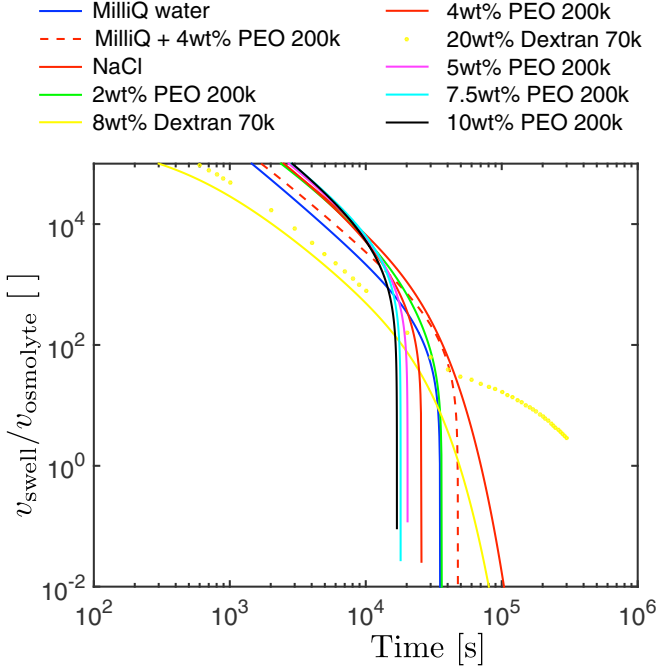


FIG. 11. Surface swelling velocity v_{swell} , the velocity at which the particle surface moves through the background liquid, normalized by the typical diffusion speed of the macromolecules $v_{\text{osmolyte}} \approx \frac{k_B T}{3\pi\eta R_g^2}$.

APPENDIX F: EQUILIBRIUM PARTITION COEFFICIENT

The equilibrium partition coefficient Q is defined as the ratio of the concentration of solute inside the hydrogel particle to the concentration outside of the particle in equilibrium. Both short-range and long-range interactions determine the equilibrium partitioning of osmolyte. Short-range interactions between the osmolyte and the hydrogel network set the fraction of available volume by determining the excluded volume through hard-core repulsive interactions. Long-range

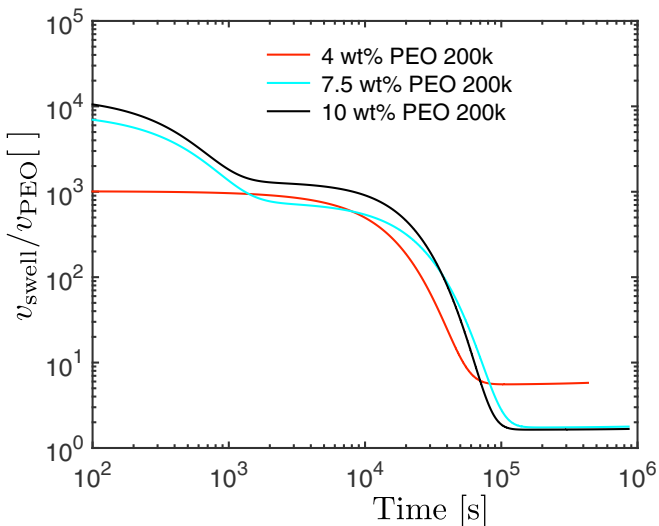


FIG. 12. Normalized compression speed in comparison with the diffusion speed of the used osmolyte.

interactions, on the other hand, set the chemical potential for osmolyte molecules in the available volume inside the hydrogel particle. In our model, we account for long-range interactions in the energetic parameter B . Therefore, we estimate Q as the fraction of available volume ϕ_{av} in the hydrogel particle, based purely on short-range interactions. Due to the finite size of osmolyte molecules, the fraction of available volume does not generally equal the equilibrium volume fraction of solvent $\phi \equiv 1 - (R_{\text{dry}}/R_{\text{eq}})^3$, with R_{dry} the radius of a fully dried hydrogel particle and R_{eq} its radius in equilibrium.

To estimate the available equilibrium volume fraction in the aquapearl hydrogels for 70k dextran, 20k PEG, and 200k PEO, we model the available volume of a hydrogel particle as being comprised of spherical solvent-filled impenetrable shells with an inner radius equal to the mesh size ξ of the hydrogel network. Assuming the osmolyte particles to be hard spheres whose radius equals their radius of gyration R_g , the available volume fraction for an osmolyte molecule in a shell equals

$$\phi_{\text{av}} = (1 - R_g/\xi)^3. \quad (\text{F1})$$

To estimate ϕ_{av} for dextran 70k, PEG 20k, and PEO 200k in the aquapearl particles, we first estimate the available volume fraction for dextran 70k using Eq. (F1). To do so, we calculate the ratio of the mesh size of the aquapearl particles ξ_{aqua} to the mesh size of a 5 wt % polyacrylamide network ξ_{poly} with known ϕ_{av} . We find the ratio of the mesh sizes by comparing the permeabilities $\kappa \propto \xi^2$ of the two kinds of hydrogel particles.

As a proxy for the available volume fraction ϕ_{av} of the 5 wt % polyacrylamide network for dextran 70k ($R_g = 6$ nm [23]), we use the measured available volume fraction of a 6 wt% polyacrylamide hydrogel for dextran molecules with a radius of 6.42 nm [28]. As a proxy for the permeability of the aquapearl particles, we use the result of Appendix D, where we found the permeability of the aquapearl particles to be $\kappa = 8(5)$ nm². To determine the permeability of 5 wt %

TABLE IV. Material properties of the soft, medium, and stiff poly-acrylamide hydrogels of Sleebom *et al.* [13] from fits with the model of the present article. For the compressive modulus of the medium and the stiff particles we used the value obtained from capillary micromechanics, see the Supplemental Material of Sleebom *et al.*, and for the soft particles we used the estimation of the compressive modulus from the fits in Sleebom *et al.* The weight percentage indicates the concentration of the dextran 70k polymer solution used in the experiment. The standard error for each derived material parameter is given in parentheses. We assumed all fitted parameters to be uncorrelated.

Experiment	Π (kPa)	K (kPa)	κ (nm ²)	D_{osm} ($\mu\text{m}^2/\text{s}$)
Medium 13 wt %	29.4	13	0.17(0.02)	1.01(0.16)
Medium 13 wt %	29.4	13	0.19(0.02)	0.74(0.11)
Medium 5 wt %	4.2	13	0.18(0.03)	3.43(0.94)
Soft 13 wt %	29.4	10	0.40(0.01)	0.51(0.02)
Soft PEG 2M	1.8	10	0.51(0.03)	0.00(0.00)
Stiff 5 wt %	4.2	17	0.15(0.09)	7.36(307.00)
Stiff 13 wt %	29.4	17	0.09(0.01)	2.46(0.34)

polyacrylamide hydrogels, we fitted our model to the compressive response of 5 wt % “medium” polyacrylamide microgel particles with dextran 70k from our previous work [13]; see Table IV for the fitted parameters. In making the fits for the medium and soft particles we enforced the particle to reswell to its original size by demanding that $BQ - P(Q - 1) = 0$, and we put $Q = \phi_{av} = 0.11$ for the medium and soft gels and $Q = \phi_{av} = 0.02$ for the stiff gels [28]. We average the fitted values for the permeability κ of the medium hydrogels to obtain an estimate for the permeability of the 5 wt % polyacrylamide network.

Assuming the proportionality constant in the scaling relation for the permeability $\kappa \propto \xi^2$ to be equal for the

polyacrylamide and the aquapearl particles, we find the ratio of the mesh size of the aquapearl particles to that of 5 wt % polyacrylamide medium hydrogels as $\xi_{aqua}/\xi_{polyac} \approx 7$. Then, using Eq. (F1), and that the available volume fraction for dextran 70k of the 5 wt % polyacrylamide hydrogels is $\phi_{av} = 0.11$ [28], we find the available volume fraction within the aquapearl particles for dextran 70k as $\phi_{av}^{dex} = 0.78$, where we used $R_g = 6$ nm [23].

As we know the ratio of the radius of PEG 20k and PEO 200k molecules to that of dextran 70k, we find the fraction of available volume for PEG 20k and PEO 200k as $\phi_{av}^{PEG} = 0.75$ and $\phi_{av}^{PEO} = 0.36$, where we used $R_g = 7$ nm for PEG 20k [24], and $R_g = 22$ nm for PEO 200k [24].

-
- [1] K. Lee and D. Mooney, Hydrogels for tissue engineering, *Chem. Rev.* **101**, 1869 (2001).
- [2] N. Peppas, P. Bures, W. Leobandung, and H. Ichikawa, Hydrogels in pharmaceutical formulations, *Eur. J. Pharm. Biopharm.* **50**, 27 (2000).
- [3] Y. Qiu and K. Park, Environment-sensitive hydrogels for drug delivery, *Adv. Drug Delivery Rev.* **53**, 321 (2001).
- [4] V. Arbona, D. Iglesias, J. Jacas, E. Primo-Millo, M. Talon, and A. Gomez-Cadenas, Hydrogel substrate amendment alleviates drought effects on young citrus plants, *Plant and Soil* **270**, 73 (2005).
- [5] S. A. Shahid, A. A. Qidwai, F. Anwar, I. Ullah, and U. Rashid, Improvement in the water retention characteristics of sandy loam soil using a newly synthesized poly(acrylamide-co-acrylic acid)/AlZnFe₂O₄ superabsorbent hydrogel nanocomposite material, *Molecules* **17**, 9397 (2012).
- [6] T. Tanaka and D. J. Fillmore, Kinetics of swelling of gels, *J. Chem. Phys.* **70**, 1214 (1979).
- [7] M. A. Biot, General theory of three-dimensional consolidation, *J. Appl. Phys.* **12**, 155 (1941).
- [8] M. Doi, Gel dynamics, *J. Phys. Soc. Jpn.* **78**, 052001 (2009).
- [9] Y. Hu, X. Zhao, J. J. Vlassak, and Z. Suo, Using indentation to characterize the poroelasticity of gels, *Appl. Phys. Lett.* **96**, 121904 (2010).
- [10] C.-Y. Hui and V. Muralidharan, Gel mechanics: A comparison of the theories of Biot and Tanaka, Hocker, and Benedek, *J. Chem. Phys.* **123**, 154905 (2005).
- [11] J. Yoon, S. Cai, Z. Suo, and R. C. Hayward, Poroelastic swelling kinetics of thin hydrogel layers: Comparison of theory and experiment, *Soft Matter* **6**, 6004 (2010).
- [12] B. Sierra-Martin, J. A. Frederick, Y. Laporte, G. Markou, J. J. Lieten-Santos, and A. Fernandez-Nieves, Determination of the bulk modulus of microgel particles, *Colloid Polym. Sci.* **289**, 721 (2011).
- [13] J. J. F. Sleebom, P. Voudouris, M. T. J. J. M. Punter, F. J. Aangenendt, D. Florea, P. van der Schoot, and H. M. Wyss, Compression and Reswelling of Microgel Particles after an Osmotic Shock, *Phys. Rev. Lett.* **119**, 098001 (2017).
- [14] B. Amsden, Solute diffusion within hydrogels: Mechanisms and models, *Macromolecules* **31**, 8382 (1998).
- [15] B. Mann, C. Holm, and K. Kremer, Swelling of polyelectrolyte networks, *J. Chem. Phys.* **122**, 154903 (2005).
- [16] A. Safronov, Y. Smirnova, G. Pollack, and F. Blyakhman, Enthalpy of swelling of potassium polyacrylate and polymethacrylate hydrogels: Evaluation of excluded-volume interaction, *Macromol. Chem. Phys.* **205**, 1431 (2004).
- [17] A. E. English, T. Tanaka, and E. R. Edelman, Polyelectrolyte hydrogel instabilities in ionic solutions, *J. Chem. Phys.* **105**, 10606 (1996).
- [18] K. Sato, T. Nakajima, T. Hisamatsu, T. Nonoyama, T. Kurokawa, and J. P. Gong, Phase-separation-induced anomalous stiffening, toughening, and self-healing of polyacrylamide gels, *Adv. Mater.* **27**, 6990 (2015).
- [19] B. Kim, K. L. Flamme, and N. A. Peppas, Dynamic swelling behavior of pH-sensitive anionic hydrogels used for protein delivery, *J. Appl. Polym. Sci.* **89**, 1606 (2003).
- [20] I. J. Suárez, A. Fernández-Nieves, and M. Márquez, Swelling kinetics of poly(n-isopropylacrylamide) minigels, *J. Phys. Chem. B* **110**, 25729 (2006).
- [21] H. Guo, N. Sanson, D. Hourdet, and A. Marcellan, Thermoresponsive toughening with crack bifurcation in phase-separated hydrogels under isochoric conditions, *Adv. Mater.* **28**, 5857 (2016).
- [22] G. Miquelard-Garnier, S. Demoures, C. Creton, and D. Hourdet, Synthesis and rheological behavior of new hydrophobically modified hydrogels with tunable properties, *Macromolecules* **39**, 8128 (2006).
- [23] C. Bonnet-Gonnet, L. Belloni, and B. Cabane, Osmotic pressure of latex dispersions, *Langmuir* **10**, 4012 (1994).
- [24] K. Devanand and J. C. Selser, Asymptotic behavior and long-range interactions in aqueous solutions of poly(ethylene oxide), *Macromolecules* **24**, 5943 (1991).
- [25] E. Díez-Peña, I. Quijada-Garrido, and J. M. Barrales-Rienda, Analysis of the swelling dynamics of cross-linked P(N-iPAAm-co-MAA) copolymers and their homopolymers under acidic medium. a kinetics interpretation of the overshooting effect, *Macromolecules* **36**, 2475 (2003).
- [26] Y. Yin, X. Ji, H. Dong, Y. Ying, and H. Zheng, Study of the swelling dynamics with overshooting effect of hydrogels based on sodium alginate-g-acrylic acid, *Carbohydr. Polym.* **71**, 682 (2008).
- [27] J. Tong and J. L. Anderson, Partitioning and diffusion of proteins and linear polymers in polyacrylamide gels, *Biophys. J.* **70**, 1505 (1996).
- [28] J. C. Williams, L. A. Mark, and S. Eichholtz, Partition and permeation of dextran in polyacrylamide gel, *Biophys. J.* **75**, 493 (1998).

- [29] P. C. Hohenberg and B. I. Halperin, Theory of dynamic critical phenomena, *Rev. Mod. Phys.* **49**, 435 (1977).
- [30] M. L. Huggins, Solutions of long chain compounds, *J. Chem. Phys.* **9**, 440 (1941).
- [31] P. J. Flory, Thermodynamics of high polymer solutions, *J. Chem. Phys.* **9**, 660 (1941).
- [32] H. O. Johansson, G. Karlstrom, F. Tjerneld, and C. A. Haynes, Driving forces for phase separation and partitioning in aqueous two-phase systems, *J. Chromatogr. B* **711**, 3 (1998).
- [33] B. N. Preston and W. D. Comper, Dextran at intermediate concentrations, *J. Chem. Soc., Faraday Trans. 1*, **78**, 1209 (1981).
- [34] R. P. Rand, Brock University, <https://tinyurl.com/y47bg7gr>.
- [35] J. Crank, *The Mathematics of Diffusion* (Clarendon Press, Oxford, 1975).
- [36] H. M. Wyss, T. Franke, E. Mele, and D. A. Weitz, Capillary micromechanics: Measuring the elasticity of microscopic soft objects, *Soft Matter* **6**, 4550 (2010).